

September 2007

# Analytical formulas and scaling laws for peak interaction forces in dynamic atomic force microscopy

Shuiqing Hu

*Purdue University - Main Campus, shuiqing@purdue.edu*

Arvind Raman

*Birck Nanotechnology Center, Purdue University, raman@purdue.edu*

Follow this and additional works at: <http://docs.lib.purdue.edu/nanopub>

---

Hu, Shuiqing and Raman, Arvind, "Analytical formulas and scaling laws for peak interaction forces in dynamic atomic force microscopy" (2007). *Birck and NCN Publications*. Paper 298.

<http://docs.lib.purdue.edu/nanopub/298>

This document has been made available through Purdue e-Pubs, a service of the Purdue University Libraries. Please contact [epubs@purdue.edu](mailto:epubs@purdue.edu) for additional information.

# Analytical formulas and scaling laws for peak interaction forces in dynamic atomic force microscopy

Shuiqing Hu and Arvind Raman<sup>a)</sup>

Birck Nanotechnology Center, School of Mechanical Engineering, Purdue University, 585 Purdue Mall, West Lafayette, Indiana 47907

(Received 2 July 2007; accepted 17 August 2007; published online 19 September 2007)

Determining the peak interaction force between an oscillating nanoscale tip and a sample surface has been a fundamental yet elusive goal in amplitude-modulated atomic force microscopy. Closed form analytical expressions are derived using nonlinear asymptotic theory for the peak attractive and repulsive forces that approximate with a high degree of accuracy the numerically simulated peak forces under ambient or vacuum conditions. Scaling laws involving van der Waals, chemical forces, nanoscale elasticity, and oscillator parameters are identified to demonstrate approximate similitude for the peak interaction forces under practical operating conditions. © 2007 American Institute of Physics. [DOI: 10.1063/1.2783226]

In dynamic atomic force microscopy (AFM), a sharp nanoscale tip on an oscillating microcantilever intermittently encounters short and long range forces while scanning over a sample during imaging, manipulation, spectroscopy, and lithography processes. The peak values of these interatomic forces are of long-standing interest in materials science and biophysics since they provide direct insight into the physics of nanoscale adhesion, viscoelasticity, and specific chemical interactions.<sup>1,2</sup> More generally, the peak forces are the imaging forces exerted by the tip on the sample and must be minimized especially while imaging soft biological matter.

However, the peak interaction force values are not directly accessible in experiments,<sup>3</sup> and predicting them from mathematical simulations<sup>4</sup> is of limited utility since the calculated values change significantly from case to case. In this letter, we present closed form analytical solutions and their scaling laws for the peak interaction forces, which approximate closely the numerically simulated values for amplitude-modulated AFM under practical experimental conditions.

We use a spherical tip-flat sample interaction model that is representative of a large class of experimental settings in ambient or vacuum conditions. The tip-sample interaction force ( $F_{ts}$ ) models attractive forces in the noncontact region and repulsive forces during contact:

$$F_{ts}(d) = \begin{cases} -\frac{C}{d^\alpha} & \text{for } d > a_0 \\ -\frac{C}{a_0^\alpha} + D(a_0 - d)^\beta & \text{for } d \leq a_0, \end{cases} \quad (1)$$

where  $C$  is a general attractive force parameter,  $d$  the instantaneous tip-sample separation,  $a_0$  the intermolecular distance at which contact is initiated and is evaluated by equating the adhesion force  $C/a_0^\alpha$  to  $2\pi R\Gamma$ , and  $\Gamma$  being the surface energy for the tip and sample materials.<sup>5</sup> This force model is fairly general; for example, (a) setting  $C=HR/6$ ,  $\alpha=2$ ,  $D=4E^*\sqrt{R/3}$ , and  $\beta=3/2$ , with  $H$ ,  $E^*$ , and  $R$  being respectively the Hamaker constant, the effective tip-sample elastic modulus, and the tip radius, we recover the well known Derjaguin-Muller-Toporov (DMT) interaction model,<sup>5</sup> where

the attractive forces arise from van der Waals forces; (b) Setting  $C=C_{\text{chemical}}$  and  $\alpha=7$  approximates attractive chemical forces under certain conditions,<sup>2</sup> and (c) letting  $D=k_{ts}$  and  $\beta=1$  models a linear repulsive interaction. These material properties are either known ( $H$ ,  $E^*$ , and  $R$ ), or can be fitted to *ab initio* calculations ( $C_{\text{chemical}}$ ), or can be measured experimentally ( $k_{ts}$ ).

The tip motion in dynamic AFM can be approximately described by a point-mass model after scaling natural time  $t$  by the driving frequency  $\omega$  ( $\tau=\omega t$ ),

$$\Omega^2 \frac{d^2x}{d\tau^2} + \frac{\Omega}{Q} \frac{dx}{d\tau} + x = \frac{F_{ts}(d)}{k_c} + \frac{F_{\text{drive}} \cos(\tau)}{k_c}, \quad (2)$$

where  $x(\tau)$  is the tip motion and  $d(\tau)$  is the instantaneous gap between the nanoscale tip and the sample [see Fig. 1(a)]. Let  $Z$  be the cantilever-sample separation so that  $d(\tau) \approx Z+x(\tau)$ .  $k_c$  is the effective stiffness of the driven mode of the microcantilever.<sup>6</sup>  $\Omega=\omega/\omega_0$ , where  $\omega_0$  is a linear resonance frequency of the cantilever, and  $Q$  is the quality factor of the chosen mode of the cantilever.  $F_{\text{drive}}$  is the magnitude of the driving force.

First, consider a numerical simulation<sup>4</sup> of Eq. (2) for the case of the DMT interaction model representing a silicon tip interacting with a soft sample. The probe is initially driven at

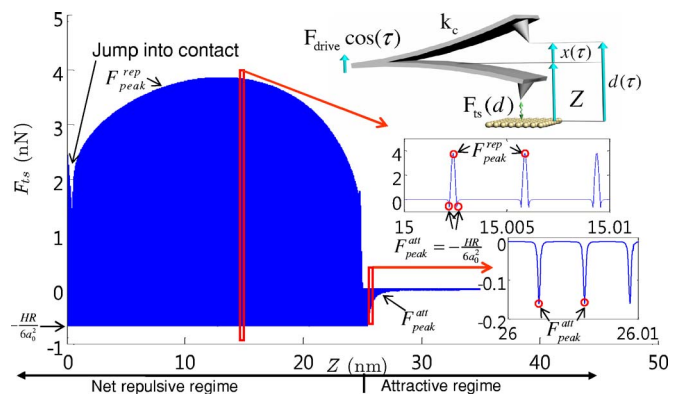


FIG. 1. (Color online) Numerically simulated tip-sample interaction forces using the DMT interaction model as  $Z$  is gradually decreased at a rate of 250 nm/s. For this simulation,  $\Omega=1$ ,  $Q=50$ ,  $A_{\text{init}}=25$  nm,  $k_c=1$  N/m,  $E^*=1$  GPa (silicon tip, soft sample),  $H=10^{-19}$  J,  $R=10$  nm, and  $a_0=0.5$  nm.

<sup>a)</sup>Electronic mail: raman@ecn.purdue.edu

an amplitude  $A_{\text{init}}$  and the interaction force history, tip oscillation amplitude  $A$ , and amplitude ratio  $A_{\text{ratio}}=A/A_{\text{init}}$  are monitored as  $Z$  is decreased. As shown in Fig. 1(a), the tip-sample interaction forces occur as short time scale spikes; our goal is to approximate analytically  $F_{\text{peak}}^{\text{att}}$  the peak attractive force in the *attractive regime* of oscillation and  $F_{\text{peak}}^{\text{rep}}$  the peak repulsive force in the *net repulsive regime* of oscillation.

Our main theoretical tool to predict the peak forces is the asymptotic theory of periodic averaging.<sup>7</sup> Briefly, this theory regards the driving, interaction, and damping forces as small perturbations to an undamped simple harmonic oscillator. The response of the oscillator is then determined from the time-averaged effects of the forces and the frequency detuning between drive and oscillator resonance frequencies. Accordingly, Eq. (2) is transformed into phase space form as follows:

$$\begin{aligned} \frac{dx}{d\tau} &= y(\tau), \\ \frac{dy}{d\tau} &= -x + \left(1 - \frac{1}{\Omega^2}\right)x - \frac{1}{\Omega Q}y + \frac{F_{\text{ts}}(d) + F_{\text{drive}} \cos(\tau)}{\Omega^2 k_c}, \end{aligned} \quad (3)$$

where  $x(\tau)$  and  $y(\tau)$  are the tip displacement and tip velocity that together are called the phase space variables. We assume that under ambient or vacuum conditions and near resonance,  $1/Q$ ,  $1-1/\Omega^2$  are also of  $O(\varepsilon)$ ,  $|\varepsilon| \ll 1$ . Furthermore, we assume that  $F_{\text{ts}}/k_c$  and  $F_{\text{drive}}/k_c$  are of  $O(\varepsilon)$  relative to the tip oscillation amplitudes.

In order to predict steady state tip amplitude  $A$  and phase  $\varphi$ , a polar transformation is introduced in Eq. (3):  $x(\tau) = A \cos(\theta)$ ,  $y(\tau) = -A \sin(\theta)$ , where  $\theta = \tau + \varphi$  and the transformed equations to  $O(\varepsilon)$  become

$$\begin{aligned} \frac{dA}{d\tau} &= \left[ -\frac{F_{\text{drive}} \cos(\varphi)}{\Omega^2 k_c} - \left(1 - \frac{1}{\Omega^2}\right)A \right] \cos(\theta) \sin(\theta) \\ &\quad - \left[ \frac{F_{\text{drive}} \sin(\varphi)}{\Omega^2 k_c} + \frac{A}{Q\Omega} \right] \sin^2(\theta) \\ &\quad - \frac{F_{\text{ts}}[Z + A \cos(\theta)]}{\Omega^2 k_c} \sin(\theta), \\ A \frac{d\varphi}{d\tau} &= \left[ -\frac{F_{\text{drive}} \cos(\varphi)}{\Omega^2 k_c} - \left(1 - \frac{1}{\Omega^2}\right)A \right] \cos^2(\theta) \\ &\quad - \left[ \frac{F_{\text{drive}} \sin(\varphi)}{\Omega^2 k_c} + \frac{A}{Q} \right] \sin(\theta) \cos(\theta) \\ &\quad - \frac{F_{\text{ts}}[Z + A \cos(\theta)]}{\Omega^2 k_c} \cos(\theta). \end{aligned} \quad (4)$$

Per our assumptions, the right hand side terms of Eq. (4) are  $O(\varepsilon)$  and Lipschitz continuous, permitting the use of the periodic averaging theorem.<sup>7</sup> Accordingly, the right hand sides of Eq. (4) are replaced by their averages from  $\theta=0$  to  $\theta=2\pi$ , leading to

$$\begin{aligned} \frac{dA}{d\tau} &= \frac{1}{2\Omega^2} \left[ -\frac{F_{\text{drive}} \sin(\varphi)}{k_c} - \frac{A\Omega}{Q} \right], \\ A \frac{d\varphi}{d\tau} &= \frac{1}{2\Omega^2} \left[ -\frac{F_{\text{drive}} \cos(\varphi)}{k_c} + (1 - \Omega^2)A \right. \\ &\quad \left. - \frac{1}{\pi k_c} \int_0^{2\pi} F_{\text{ts}}[Z + A \cos(\theta)] \cos(\theta) d\theta \right]. \end{aligned} \quad (5)$$

Setting  $dA/d\tau$  and  $d\varphi/d\tau$  to zero for steady state oscillations, eliminating the phase  $\varphi$  between the two resulting equations, and noting that  $F_{\text{drive}}^2/k_c^2 = A_{\text{init}}^2[(\Omega^2/Q^2) + (1 - \Omega^2)^2]$  far from the sample leads to

$$\begin{aligned} A_{\text{ratio}}^2 &= \left( \frac{A}{A_{\text{init}}} \right)^2 = \frac{\Omega^2 + Q^2(1 - \Omega^2)^2}{\Omega^2 + Q^2(\omega_e^2 - \Omega^2)^2}, \\ \omega_e^2 &= 1 - \frac{1}{\pi k_c A} \int_0^{2\pi} F_{\text{ts}}[Z + A \cos(\theta)] \cos(\theta) d\theta, \end{aligned} \quad (6)$$

where  $\omega_e$  is the *nonlinear resonance frequency* of the probe at a separation of  $Z$  and oscillating with amplitude  $A$ . The expression for  $\omega_e$  is identical to the one used in frequency-modulated AFM.<sup>2</sup> Equation (6), thus, states that amplitude reduction in amplitude-modulated AFM occurs due to the detuning between the drive and the *nonlinear* tip resonance frequencies.

We begin by computing the  $F_{\text{peak}}^{\text{att}}$  when the tip is in the attractive regime of oscillation. First, consider a van der Waals interaction model  $F_{\text{ts}}(d) = -HR/6d^2$  which can be substituted into Eq. (6) to find  $Z$  as a function of  $A$ . Of the three solutions possible, the physically meaningful stable solution is such that  $Z \approx A$ . Using this simplification, solving for  $A$ , and noting that  $F_{\text{peak}}^{\text{att}} = F_{\text{ts}}[Z - A]$  leads to a closed form expression for  $F_{\text{peak}}^{\text{att}}$  at  $\Omega = 1$ ,

$$\begin{aligned} \bar{F}_{\text{peak}}^{\text{att}} &= (HR)^{1/3} (Q/k_c)^{4/3} A_{\text{init}}^{-2} F_{\text{peak}}^{\text{att}} = -2 \cdot 3^{(1/3)} (A_{\text{ratio}} \\ &\quad - A_{\text{ratio}}^3)^{2/3}, \end{aligned} \quad (7)$$

where  $\bar{F}_{\text{peak}}^{\text{att}}$  is the nondimensional peak attractive force. A similar procedure for attractive chemical interaction forces,  $F_{\text{ts}} = -C_{\text{chemical}}/d^7$  (Ref. 2) at  $\Omega = 1$  leads to

$$\begin{aligned} \bar{F}_{\text{peak}}^{\text{att}} &= C_{\text{chemical}}^{1/13} (Q/k_c)^{14/13} A_{\text{init}}^{-21/13} F_{\text{peak}}^{\text{att}} = -2^{(133/13)} \\ &\quad \times 231^{(-14/13)} (A_{\text{ratio}} - A_{\text{ratio}}^3)^{7/13}, \end{aligned} \quad (8)$$

where  $\bar{F}_{\text{peak}}^{\text{att}}$  is now the nondimensional peak attractive force expression for this specific chemical force model. Not surprisingly, the method above can be extended to any attractive interaction force that is adequately described by a power law, and also for cases where  $\Omega \neq 1$ .

In order to derive an analytical relation for the  $F_{\text{peak}}^{\text{rep}}$ , one needs insightful approximations of the integrand for  $\omega_e$  [Eq. (6)] in the net repulsive regime of oscillation. If, for instance, the contributions of the attractive forces to  $F_{\text{peak}}^{\text{rep}}$  are negligible, then expanding the integrand in a series about  $\theta = \pi$  for small normalized maximum indentation  $\delta = (a_0 + A - Z)/Z$  leads to

$$\omega_c^2 \approx 1 + \frac{4\sqrt{2E^*RA_{\text{init}}A_{\text{ratio}}}}{3\pi k_c} \left( \frac{a_0 + A - Z}{Z} \right)^2. \quad (9)$$

Substituting this equation into Eq. (6), solving  $Z$  as a function of  $A_{\text{ratio}}$ , and substituting the resulting equation into Eq. (1) leads to (for  $\Omega=1$ )

$$\begin{aligned} \bar{F}_{\text{peak}}^{\text{rep}} &= (E^*\sqrt{R})^{-1/4} (Q/k_c)^{3/4} A_{\text{init}}^{-9/8} F_{\text{peak}}^{\text{rep}} = 2^{(1/8)} 3^{-(1/4)} \pi^{(3/4)} \\ &\times (A_{\text{ratio}} - A_{\text{ratio}}^3)^{3/8}, \end{aligned} \quad (10)$$

where  $\bar{F}_{\text{peak}}^{\text{rep}}$  is the nondimensional value of  $F_{\text{peak}}^{\text{rep}}$ . If the sample elasticity is unknown, then an equivalent tip-sample contact spring stiffness  $k_{ts}$  can be measured experimentally. In this case,  $D=k_{ts}$  and  $\beta=1$ , and following the derivation above, we get (for  $\Omega=1$ )

$$\begin{aligned} \bar{F}_{\text{peak}}^{\text{rep}} &= k_{ts}^{-1/3} (Q/k_c)^{2/3} A_{\text{init}}^{-1} F_{\text{peak}}^{\text{rep}} = 2^{-(5/3)} 3^{(2/3)} \pi^{(2/3)} (A_{\text{ratio}} \\ &- A_{\text{ratio}}^3)^{1/3}. \end{aligned} \quad (11)$$

To verify the theoretical predictions for  $F_{\text{peak}}^{\text{att}}$  and  $F_{\text{peak}}^{\text{rep}}$  [Eqs. (7) and (10)], 600 simulations are performed with the DMT interaction model for every combination of four  $k_c$  values with associated three  $Q$  values: for  $k_c=1$  N/m,  $Q=50, 75$ , and  $100$ ; for  $k_c=10$  N/m,  $Q=250, 400$ , and  $550$ ; for  $k_c=40$  N/m,  $Q=300, 550$ , and  $800$ ; for  $k_c=140$  N/m,  $Q=700, 1000$ , and  $1300$ ; and for  $k_c=200$  N/m,  $Q=900, 1300$ , and  $1700$ . For each  $k_c, Q$  combination above, simulations are performed for  $A_{\text{init}}=10, 25, 50$ , and  $100$  nm;  $E^*=0.01, 0.1, 1, 10$ , and  $100$  GPa; and  $H=10^{-19}$  and  $10^{-20}$  J.  $R$  and  $a_0$  vary less than an order of magnitude in practice and are kept constant at typical values of  $10$  and  $0.5$  nm. This range of parameters encompasses most commercially available dynamic AFM probes operating in air, as well as operating conditions and material properties of interest. In Figs. 2(a) and 2(b), the  $F_{\text{peak}}^{\text{att}}$  and  $F_{\text{peak}}^{\text{rep}}$  values from these 600 simulations are scaled according to Eqs. (7) and (10), and plotted against  $A_{\text{ratio}}$ . Clearly, 95% of the simulated  $\bar{F}_{\text{peak}}^{\text{att}}$  and  $\bar{F}_{\text{peak}}^{\text{rep}}$  values collapse to within 10% of the theoretically predicted, *quasiuniversal* curves. As shown in Fig. 2(c), the analytically predicted  $\bar{F}_{\text{peak}}^{\text{rep}}$  using Eq. (10) compares excellently with numerical simulations in prior work.<sup>5</sup>

Additional simulations have been performed with probes typically used in vacuum applications, and the match between the analytical expression and numerical simulation is excellent. Furthermore, the inclusion of small to moderate sample viscoelasticity does not influence significantly the match between analytical prediction and numerical simulations. However, the present approach cannot be applied directly for predicting peak forces in liquid environments.<sup>8</sup>

In conclusion, we have presented closed form, analytical formulas and their scaling laws for peak interaction forces using different attractive and repulsive tip-sample interaction models. The ability of the formulas to predict peak forces under practical ambient and vacuum conditions is remarkable given the complex nonlinear phenomena that underpin dynamic AFM.<sup>9</sup> The approximate scaling laws suggest that (1)  $F_{\text{peak}}^{\text{rep}}$  depends on local sample elasticity or stiffness,

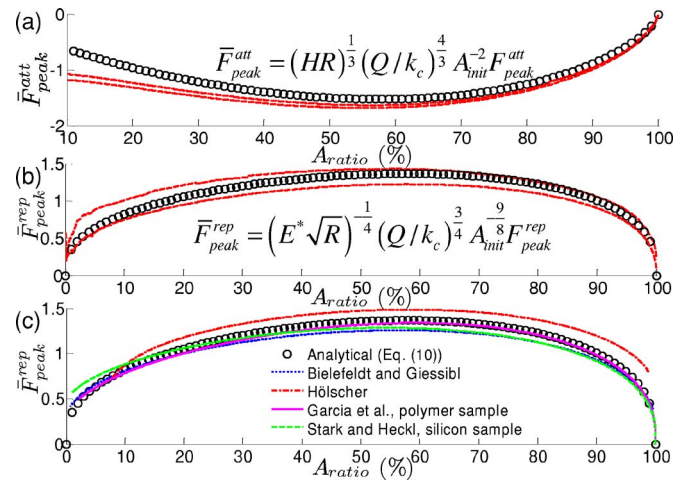


FIG. 2. (Color online) [(a) and (b)] 95% confidence interval bounds (dashed lines) of the 600 numerically simulated nondimensional peak force values as a function of the amplitude ratio  $A_{\text{ratio}}$  with DMT interaction model for  $\bar{F}_{\text{peak}}^{\text{att}}$ ,  $\bar{F}_{\text{peak}}^{\text{rep}}$ . (c)  $\bar{F}_{\text{peak}}^{\text{rep}}$  values using Eq. (10) are compared with numerical simulation results using the parameters given in prior literature (Ref. 5).

while  $F_{\text{peak}}^{\text{att}}$  depends on local attractive force constants. Consequently, peak forces cannot be constant during a scan in amplitude-modulated AFM, where the  $A_{\text{ratio}}$  is kept constant during the imaging process. (2) The physical parameters and operating conditions that have the most influence on peak forces can be identified based on the power laws in the analytical formulas. They are, in decreasing order of importance,  $A_{\text{ratio}}$  and  $A_{\text{init}}$  (operating conditions), followed by the ratio  $k_c/Q$  (oscillator parameters), then by  $E^*$ ,  $k_{ts}$ ,  $H$ ,  $C_{\text{chemical}}$  (tip-sample material properties), and lastly, by  $R$  (tip geometry). The simplicity and accuracy of the scaling laws make them ideal for experimentalists interested in a quantitative understanding of imaging forces applied to the sample in dynamic AFM.

The authors wish to thank the National Science Foundation for research funding provided under Grant No. CMMI 0409660, and R. Reifengerger (Physics, Purdue) for insightful discussions on the topic.

<sup>1</sup>J. P. Cleveland, B. Anczykowski, A. E. Schmid, and V. B. Elings, Appl. Phys. Lett. **72**, 2613 (1998).

<sup>2</sup>F. J. Giessibl, Phys. Rev. B **56**, 16010 (1997).

<sup>3</sup>M. Stark, R. W. Stark, W. M. Heckl, and R. Guckenberger, Proc. Natl. Acad. Sci. U.S.A. **99**, 8473 (2002); J. Legleiter, M. Park, B. Cusick, and T. Kowalewski, *ibid.* **103**, 4813 (2006).

<sup>4</sup>VEDA (Virtual Environment for Dynamic AFM): Dynamic Approach Curves, <http://www.nanohub.org/>

<sup>5</sup>H. Bielefeldt and F. J. Giessibl, Surf. Sci. **440**, 863 (1999); Hölscher, Appl. Phys. Lett. **89**, 123109 (2006); Fig. 2(c) in R. Garcia, C. J. Gomez, N. F. Martinez, S. Patil, C. Dietz, and R. Magerle, Phys. Rev. Lett. **97**, 016103 (2006); R. W. Stark and W. M. Heckl, Surf. Sci. **457**, 219 (2000).

<sup>6</sup>J. Melcher, S. Hu, and A. Raman, Appl. Phys. Lett. **91**, 053101 (2007).

<sup>7</sup>J. A. Sanders and F. Verhulst, *Averaging Methods in Nonlinear Dynamical Systems* (Springer, New York, 1985).

<sup>8</sup>S. Basak and A. Raman, Appl. Phys. Lett. **91**, 064107 (2007).

<sup>9</sup>S. Hu and A. Raman, Phys. Rev. Lett. **96**, 036107 (2006); S. Rutzel, S. I. Lee, and A. Raman, Proc. R. Soc. London, Ser. A **459**, 1925 (2003).